J Therm Anal Calorim (2010) 99:27–31
DOI 10.1007/s10973-009-0462-0

The effect of specific surface area of TiO_2 on the thermal decomposition of ammonium perchlorate

Kaori Fujimura · Atsumi Miyake

Japan Symposium 2008

Abstract The thermal decomposition of ammonium perchlorate (AP) is considered to be the first step in the combustion of AP-based composite propellants. In this report, the effect of the specific surface area of titanium oxide (TiO_2) catalysts on the thermal decomposition characteristics of AP was examined with a series of thermal analysis experiments. It was clear that the thermal decomposition temperature of AP decreased when the specific surface area of TiO_2 increased. It was also possible that TiO_2 influences the frequency factor of AP decomposition because there was no observable effect on the activation energy.

Keywords Ammonium perchlorate · Specific surface area · Thermal decomposition · Titanium oxide

Introduction

Burning rate and specific impulse are representative parameters that describe the burning characteristics of solid propellants. In order to design rocket motors, the basic method to satisfy the required relationship between impulse and combustion time of the rocket motor is the adjustment of the burning area by tailoring the grain configuration of the propellant. However, controlling the burning rate more widely would be very advantageous in designing rocket motors because the restriction on grain configuration could be lessened. Representative methods to control the burning rate of composite solid propellants used to date include adding a combustion catalyst [1–10] and controlling the particle size of the solid oxidizer [11, 12].

It is well known that the burning rate of these composite propellants which consist of ammonium perchlorate (AP) is enhanced when some transition metal oxides (TMOs) are added to the compositions [1–3, 6, 7]. For example, ferric oxide (Fe_2O_3), copper oxide (CuO or Cu_2O), copper chromate ($CuCrO_4$), copper chromite ($CuCr_2O_4$), and manganese oxide (MnO_2) are very effective in enhancing the burning rate. Although many researchers have proposed various theories as to how TMOs enhance the burning rate, the mechanism remains unclear. It also has been observed that the specific surface area of the combustion catalysts greatly affects the burning rate enhancement. However, there have been few studies in which the effect of specific surface area was confirmed experimentally. Recently, nano-sized particles have become available at a relatively low price, but there have been few reports of these nano-sized particles applied to composite propellants as combustion catalysts [8–10].

In a previous report, the effect of the particle size of ferric oxide (Fe_2O_3) catalysts on the thermal decomposition of AP-based composite propellants and pure AP was examined with a series of thermal analysis experiments [1]. It was clear that the thermal decomposition of the propellant samples and pure AP was greatly enhanced by reducing the size of Fe_2O_3 from the submicron to nanometer size. Recently, it has been reported that titanium oxide (TiO_2) nanoparticles enhanced the burning rate of AP-based solid composite propellants [10]. In the present study, the thermal decomposition characteristics of AP, which has been considered to be the first step of AP-based propellant decomposition, with and without TiO_2 catalysts were determined, and the effect of the specific surface area

K. Fujimura (✉) · A. Miyake
Yokohama National University, 79-7 Tokiwadai, Hodogayaku, Yokohama, Kanagawa 240-8501, Japan
e-mail: d07tf008@ynu.ac.jp

of the TiO_2 catalysts on the AP decomposition was investigated by thermal analyses.

Experimental

Materials

The particle size of AP used in this study was about 10 μm. Five types of commercial TiO_2 particles were used as catalysts and their specifications are listed in Table 1. The specific surface areas of TiO_2 in Table 1 were experimentally confirmed by the BET method with an automatic surface area analyzer, Betasorb model 4200 (Nikkiso Co., Ltd.).

In order to prepare the samples for thermal analysis, AP and each TiO_2 powder were heated separately at 120 °C for 3 h in a furnace to eliminate moisture. The designated weights of AP and TiO_2 were measured, and the samples were thoroughly mixed with a wooden stick in a mortar. The ratio of AP and TiO_2 in the samples was 97:3.

Thermal analysis

Differential scanning calorimetry (DSC) measurements were carried out with a DSC 822_e differential scanning calorimeter (Mettler-Toledo K. K.). The sample was placed in an aluminum pan and then the pan was sealed to withstand an internal pressure of about 3 MPa. The weight of the sample was about 1.0 mg. Dynamic scans were performed at a heating rate of 10 °C min^{-1} in a temperature range from 20 to 500 °C. During the measurement, nitrogen gas was purged throughout the system at 50 mL min^{-1} to maintain an inert environment.

Thermogravimetric (TG) analyses and differential thermogravimetry (DTG) measurements were carried out with a TGA/SDTA 851_e thermogravimetric analyzer (Mettler-Toledo K. K.). The sample (about 3.0 mg) was placed in an open-type alumina pan. The dynamic scans were performed at a heating rate of 3, 5, 8, and 10 °C min^{-1}, in a temperature range from 30 to 600 °C. During the measurement, nitrogen gas was purged throughout the system at 200 mL min^{-1} to maintain an inert environment. Each sample was measured three times. For both instruments, the $Star_e$ software (Mettler-Toledo K. K.) was used to control the temperature program and obtain thermograms for analysis.

Results and discussion

Thermal analysis

The DSC curves of the samples at a heating rate of 10 °C min^{-1} are shown in Fig. 1. Two thermal events are observed in each curve: a small endothermic peak near 240 °C and a large exothermic peak around 450 °C. The peak temperatures were measured at least three times per sample and then averaged. The endothermic peak near 240 °C is attributed to the phase transition of AP from the orthorhombic to cubic form [13, 14]. The relationship between the peak temperature T_p of the large exothermic peak around 450 °C and the specific surface area of the TiO_2 catalyst is summarized in Fig. 2. The peak temperatures of the samples including TiO_2 were nearly equivalent to that of pure AP, showing the peak temperature did not depend on the surface area of the TiO_2 catalyst. One explanation for these results is that the reaction between AP and TiO_2 catalyst is depressed, because the sample pans used in the DSC experiment were sealed completely, compressing the reaction gas inside the pan.

The TG and DTG curves at a heating rate of 10 °C min^{-1} are shown in Fig. 3. α is the conversion degree as represented below [15]:

$$\alpha = \frac{m(t=0) - m(t)}{m(t=0) - m(t \to \infty)} \quad (1)$$

All DTG curves consisted of a small peak and a large peak. It has been pointed out that AP decomposition occurs in two steps: low temperature decomposition (LTD) (<350 °C) and high temperature decomposition (HTD) (>350 °C) [16–18]. The first peak indicates the LTD of AP. For every sample, the LTD reaction starts near 300 °C and then shows a shoulder near 340 °C in the DTG curve. This peak cannot be observed in the DSC curve. The reaction is

Table 1 Specifications of TiO_2 particles

TiO_2(IV)	Manufacturer	Particle size (from catalogs)/nm	Specific surface area (BET method)/m^2 g^{-1}
(A)	Wako Pure Chemical Industries, Ltd.	<5000	55
(B)	Kanto Chemical Co., Inc.	19.7–101.0	35
(C)	Kanto Chemical Co., Inc.	200	18
(D)	Wako Pure Chemical Industries, Ltd.	<5000	7
(E)	Kanto Chemical Co., Inc.	100–300	6

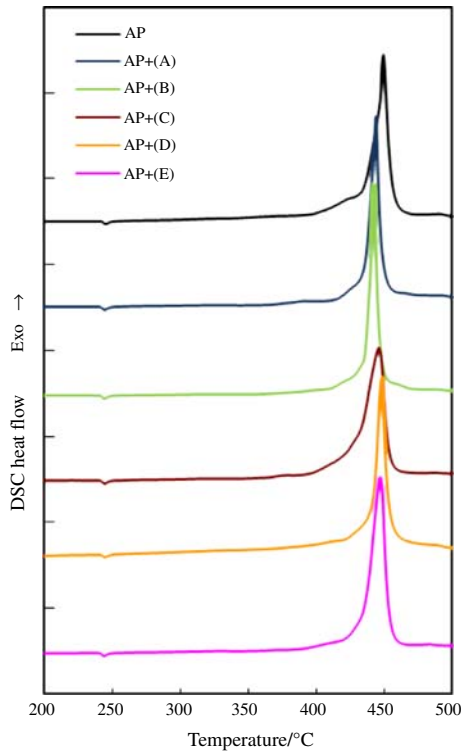

Fig. 1 DSC curves of pure AP and mixtures of AP with TiO_2 catalysts (heating rate: 10 °C min^{-1})

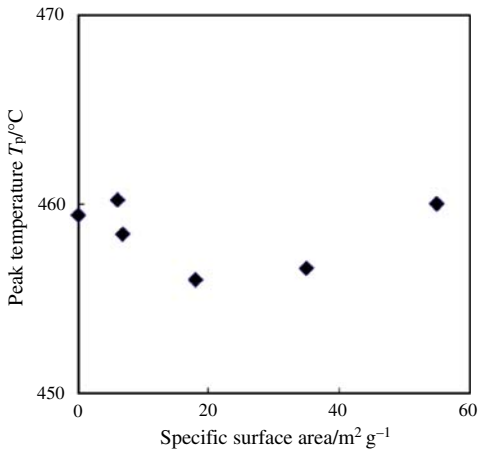

Fig. 2 The relationship between the peak temperature T_p of the large exothermic peak around 450 °C and the specific surface area of TiO_2 catalyst

depressed by the pressurization from the sealing of the sample pan in the DSC experiment, so that the peak may be shifted to higher temperature and overlapped with the next peak. Boldyrev proposed that this LTD reaction starts with nucleation followed by proton transfer as shown below [16],

$$NH_4ClO_4(s) \rightleftarrows NH_3(g) + HClO_4(g) \quad (2)$$

From the TG results, it was concluded that the LTD reaction was not affected by TiO_2 catalysts.

The next large peak indicates the HTD of AP. Boldyrev showed that the HTD starts from the dissociation of AP into NH_3 and $HClO_4$ on the surface of AP, then secondary reactions between the thermal decomposition products of $HClO_4$ and NH_3 occur either on the surface of AP or in the gas phase above the surface [16]. In the presence of TiO_2 catalyst, it can be seen that both onset temperature and peak temperature are lower than those of pure AP. The relationship between the peak temperature of HTD of AP and the specific surface area of TiO_2 catalyst is summarized in Fig. 4. The temperature shift of this peak increases as the specific surface area of TiO_2 gets larger and the plot is found to be linear except for pure AP (the specific surface area of $TiO_2 = 0$). Therefore, it can be concluded that this HTD reaction of AP takes place on the surface of the TiO_2 catalyst.

Kinetic analysis

Kinetic analyses were carried out by the Ozawa method, which is known as a model-free approach [19]. It is also known as an iso-conversional method. In order to determine the activation energy of HTD of AP using TG data, it is assumed that each reaction follows the Arrhenius equation,

$$k = A\exp(-E_a/RT) \quad (3)$$

where k is the rate constant, E_a is the activation energy, R is the gas constant, T is the absolute temperature, and A is the frequency factor. $g(\alpha)$ can be defined as the integral function of conversion degree as shown below,

$$g(\alpha) = \int_0^{\alpha} \frac{d\alpha}{f(\alpha)} = kt \qquad \left(\because \frac{d\alpha}{dt} = kf(\alpha)\right) \quad (4)$$

In this case, the thermal stability of the samples at various heating rates can be analyzed using a Ozawa plot in which $\log \beta$ versus $1/T$ shows a linear relationship, as shown in the following equation:

$$\log \beta = \log \frac{AE_a}{g(\alpha)} - 2.315 - 0.4567\frac{E_a}{RT} \quad (5)$$

where β is the heating rate [19]. When $\log \beta$ is plotted against $1/T$ for each of $\alpha =$ constant, a straight line is obtained with a slope equal to $-0.4567E_a/RT$, and then E_a can be calculated.

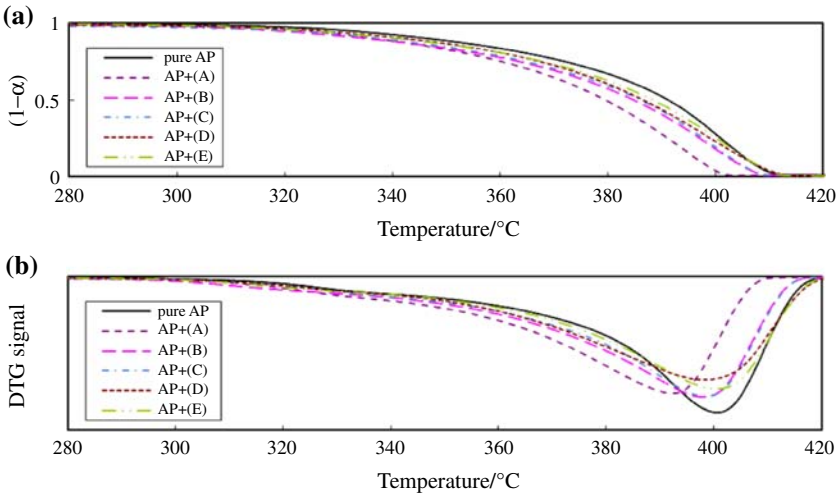

Fig. 3 **a** TG curves of pure AP and mixtures of AP with TiO_2 catalysts. **b** DTG curves of pure AP and mixtures of AP with TiO_2 catalysts (heating rate: 10 °C min^{-1})

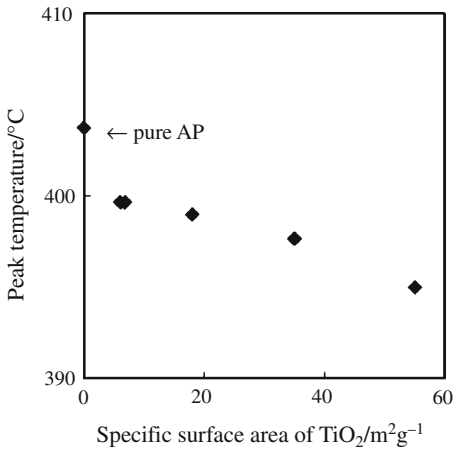

Fig. 4 The relationship between the peak temperature of HTD of AP in DTG curves and the specific surface area of TiO_2 catalyst

The activation energy for $\alpha = 0.5$ which represents the HTD reaction calculated by Ozawa plots and its correlation coefficient (r) are summarized in Table 2. The difference in the activation energy between pure AP and AP+ various TiO_2 is negligible regardless of the specific surface area. Therefore, we conclude that the specific surface area of the TiO_2 catalyst does not influence the activation energy of the HTD reaction of AP. In other words, the energy required for the HTD reaction to occur is not affected by either the specific surface area of TiO_2 or the existence of TiO_2.

Table 2 Activation energy of HTD reaction of AP calculated with the Ozawa method

Sample	E_a/kJ mol^{-1}	r
Pure AP	124	0.957
AP + (A)	115	0.929
AP + (B)	123	0.970
AP + (C)	139	0.978
AP + (D)	133	0.965
AP + (E)	123	0.919

The frequency factor A could not be determined, because the method used above is the model-free approach and no kinetic model is taken into account. Given the fact that the TiO_2 catalyst does not influence the activation energy but decreases the reaction temperature with increasing specific surface area, there is a possibility that TiO_2 affects the frequency factor. This warrants further study.

Conclusions

It was clear that the thermal decomposition of AP was enhanced by increasing the specific surface area of TiO_2. In particular, the effect on the HTD of AP is apparent and there is a linear relationship between the peak temperature of HTD of AP in DTG curves and the specific surface area of the TiO_2 catalyst. It is also possible that the TiO_2 influences the frequency factor of AP decomposition because there was no observable effect on the activation energy.

Acknowledgements This research was supported by the Technical Research & Development Institute at the Ministry of Defense. We would also like to acknowledge Professor Kohga of the National Defense Academy for his assistance and advice on performing specific surface area measurements.

References

1. Fujimura K, Miyake A. Sci Technol Energ Mater. 2008;69:149.
2. Krishnan S, Jeenu R. Combustion characteristics of AP/HTPB propellants with burning rate modifiers. J Propuls Power. 1992;8:748–55.
3. Chakravarthy SR, Price EW, Sigmant RK. Mechanism of burning rate enhancement of composite solid propellants by ferric oxide. J Propuls Power. 1997;13:471–80.

4. Fong CW, Hamshere BL. The mechanism of burning rate catalysis in. Composite HTPB-AP propellant combustion. Combust Flame. 1986;65:61–9.
5. Fong CW, Hamshere BL. The mechanism of burning rate catalysis incomposite propellants by transition-metal complexes. Combust Flame. 1986;65:71–8.
6. Dubey BL, Nath N, Tripathi A, Tiwari N. Catalysed. combustion of ammonium perchlorate, polystyrene and their composite propellants. Indian J Eng Mater Sci. 1994;1:341–9.
7. Pearson GS. Composite propellant catalysts: copper chromate and chromite. Combust Flame. 1970;14:73–84.
8. Patil PR, Krishnamurthy VN, Joshi SS. Differential scanning calorimetric study of HTPB based composite propellants in presence of nano ferric oxide. Propellants Explos Pyrotech. 2006;6: 442–6.
9. Li W, Cheng H. Cu-Cr-O nanocomposites: synthesis and characterization as catalysts for solid state propellants. Solid State Sci. 2007;9:750–5.
10. Small JL, Stephens MA, Deshpande S, Peterson EL, Seal S. Proceedings of 20th International Colloquium on the Dynamics of Explosions and Reactive Systems, Montreal, July 31–August 5, 2005.
11. Pivkina A, Frolov Yu, Ivanov D. Nanosized components of energetic systems: structure, thermal behavior, and combustion. Combust Expl Shock Waves. 2007;43:51–5.
12. van der Heijden AEDM, Leeuwenburgh AB. HNF/HTPB propellants: influence of HNF particle size on ballistic properties. Combust Flame. 2009;156:1359–64.
13. Shen SH, Chen SI, Wu BH. The thermal decomposition of ammonium perchlorate (AP) containing a burning-rate modifier. Thermochim Acta. 1993;223:135–43.
14. Rocco JAFF, Lima JES, Frutuoso AG, Iha K, Ionashiro M, Matos JR, et al. Thermal degradation of a composite solid propellant examined by DSC. J Therm Anal Calorim. 2004;75:551–7.
15. Longuet B, Gillard P. Experimental investigation on the heterogeneous kinetic process of the low thermal decomposition of ammonium perchlorate particles. Propellants Explos Pyrotech. 2009;34:59–71.
16. Boldyrev VV. Thermal decomposition of ammonium perchlorate. Thermochim Acta. 2006;443:1–36.
17. Halawy SA, Al-Shihry SS. Role of the acidic-basic characters of some metal oxides in the pyrolysis of ammonium perchlorate. J Therm Anal Calorim. 1999;55:833–40.
18. Chen L-J, Li G-S, Qi P, Li L-P. Thermal decomposition of ammonium perchlorate activated via addition of NiO nanocrystals. J Therm Anal Calorim. 2008;92:765–9.
19. Ozawa T. Kinetic analysis of derivative curves in thermal analysis. J Therm Anal Calorim. 1970;2:301–24.